

Notes

Melting Point and Domain Size of PVIBE/ ϵ -PL/Saponite Clay Investigated by Solid-State ^{13}C NMR

Atsushi Asano,* Chikako Tanaka, and Takuzo Kurotsu

Department of Applied Chemistry, National Defense Academy, Yokosuka 239-8686, Japan

Received July 8, 2008

Revised Manuscript Received October 13, 2008

Introduction

According to the Gibbs–Thomson effect,¹ melting point (T_m) of crystalline phase depends on the lamellar thickness: the thicker lamellar exhibits the higher T_m . On the other hand, the depression of T_m is also observed for a miscible polymer blend of a semicrystalline polymer and an amorphous polymer. This phenomenon is known as a diluent effect by mixing with the miscible amorphous polymer.² The rate of crystallization becomes slow, and the growth of crystalline phase is hindered. If the decrease of T_m is mainly governed by the diluent effect, the crystallinity is also supposed to decrease with increase of composition. On the other hand, in the case of the Gibbs–Thomson effect, the degree of the crystallinity remains unchanged but the lamellar thickness decreases.

In our previous study,³ we have showed that the T_m of semicrystalline poly(ϵ -L-lysine) (ϵ -PL) shifts toward lower temperature after blending with semicrystalline poly(vinyl isobutyl ether) (PVIBE), and the degree of T_m shift depends on the composition as shown in Figure 1B. In contrast, Figure 1A shows that the glass transition temperature (T_g) and the T_m of PVIBE do not change in the blends. We interpreted the T_m shift of ϵ -PL as the Gibbs–Thomson effect because the estimated total lamellar thickness of ϵ -PL in the PVIBE/ ϵ -PL blends from NMR showed a good relationship with the shift of T_m .³ Furthermore, the degree of crystallinity of ϵ -PL was approximately constant except for the PVIBE/ ϵ -PL=10/1 blend (see Table 1). However, there still remains an argument on whether the diluent effect of adding PVIBE is predominant or not because T_m of PVIBE (ca. 315 K) is much lower than that of ϵ -PL (ca. 445 K).

In this Note, we focus on the T_m of ϵ -PL for the blends and its saponite clay nanocomposites. We found that the T_m of ϵ -PL does not depend on the composition by adding synthetic saponite clay.

Experimental Section

Materials. Semicrystalline and microbial produced poly(ϵ -L-lysine) (ϵ -PL) was provided from Chisso Corp. as a solid powder, and its repeating unit is $-\text{NHCH}_2\text{CH}_2\text{CH}_2\text{CH}_2\text{CH}(\text{NH})\text{CO}-$. The relative weight-average molecular weight, M_w , is ~ 4700 , and the degree of the crystallinity, x_c , obtained from NMR is ca. 60%.⁴ Semicrystalline poly(vinyl isobutyl ether) (PVIBE) was obtained

from Scientific Polymer Products, Inc., and the repeating unit is $-\text{CH}_2\text{CH}(\text{OCH}_2\text{CH}(\text{CH}_3)_2)-$. The values of M_w and x_c are 600 000 and ca. 20%, respectively.³ Saponite clay was obtained from Kunimine Industries Co., Ltd. Saponite is synthetic and a kind of smectite clay. It has a relatively small aspect ratio rather than that of montmorillonite clay. Furthermore, it has no paramagnetic center such as Fe^{3+} .

Blends and Nanocomposites Preparation. The PVIBE/ ϵ -PL blends and its nanocomposites with saponite clay were obtained from the solvent-cast method from chloroform/methanol = 9/1 (volume ratio) mixed solution dissolved those polymers at a concentration of 15% (w/v). In order to make the saponite clay layers to be exfoliated, the saponite clay dissolved in ϵ -PL water solution with 3 wt % concentration prior to mix with PVIBE; hereafter we represent the composition by weight ratio as ϵ -PL/saponite clay = 1/0.03. The saponite clay/ ϵ -PL mixed powder was obtained by drying the ϵ -PL water solution. The obtained blends and nanocomposites were further dried under vacuum at 313 K for over 24 h.

NMR. ^{13}C NMR measurements were made using a Bruker DMX500 spectrometer operating at 125.76 MHz for ^{13}C and 500.13 MHz for ^1H . High-resolution solid-state ^{13}C NMR spectra were obtained by the combined use of cross-polarization (CP) and magic-angle spinning (MAS) with ^1H high-power dipolar decoupling of 56 kHz. ^{13}C chemical shifts were measured relative to tetramethylsilane (TMS) using the methine carbon signal at 29.47 ppm for solid adamantane as an external standard. The ^1H spin–lattice relaxation times in the laboratory frame (T_1^{H}) was indirectly measured from well-resolved ^{13}C signals enhanced by CP of 800 μs applied after the inversion–recovery pulse sequence for ^1H .

DSC. The differential scanning calorimetry (DSC) was examined by using a Perkin-Elmer 7 system with increasing temperature at rate of 2 K min^{-1} from 233 to 473 K.

Results and Discussion

Figure 1 shows the DSC results of the PVIBE/ ϵ -PL blends and the PVIBE/ ϵ -PL/saponite clay nanocomposites. Figure 1A represents T_g and T_m thermal transitions of PVIBE in the blends. The thermal transitions of PVIBE show no change after blending. These features were also observed in the nanocomposites. Parts B and C of Figure 1 show T_m of ϵ -PL for the PVIBE/ ϵ -PL blends and the PVIBE/ ϵ -PL/saponite nanocomposites, respectively.

Figure 1B shows that the T_m transition has two distinct peaks at 445 K as a sharp line and at 438 K as a broad line, and the relative intensity of the sharp peak decreases largely after blending. This may indicate that ϵ -PL consists of two different crystalline phases, and the relative ratio is changed upon blending. Here, we do not touch upon the detail of the difference in the crystalline phase in this study but focus on the transition temperature. The T_m peak shifts toward lower temperature with increasing of the PVIBE composition. This phenomenon is successfully explained by the Gibbs–Thomson relation in our previous paper.³

Two T_m peaks for ϵ -PL/saponite clay = 1/0.03 appeared at 442 and 457 K as shown in Figure 1C. This is due to the difference in sample preparation. The ϵ -PL/saponite clay =

* Corresponding author: Tel 81-46-841-3810; Fax 81-46-844-5901; e-mail asanoa@nda.ac.jp.

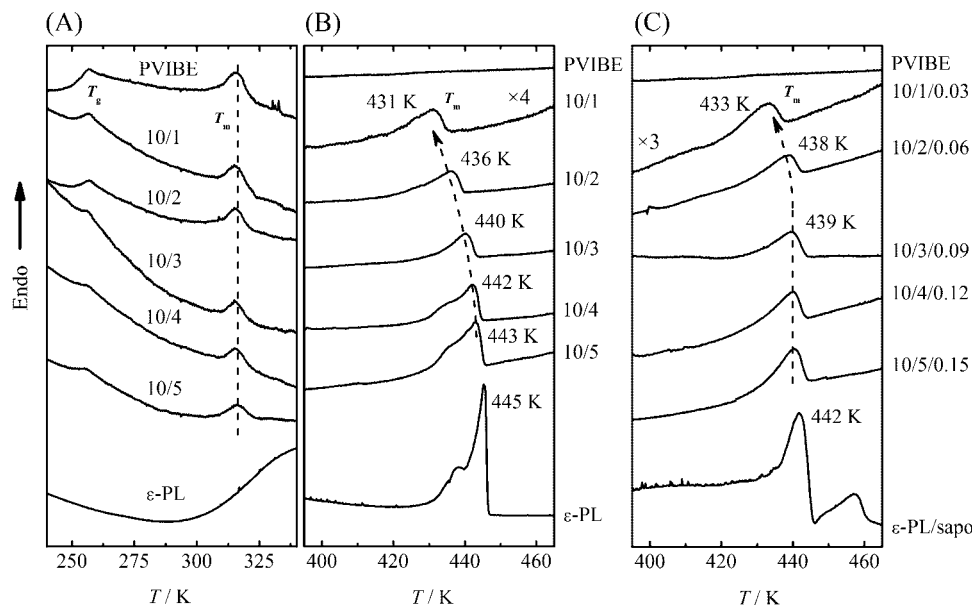


Figure 1. DSC curves of PVIBE/ ϵ -PL blends (A and B) and PVIBE/ ϵ -PL/saponite clay nanocomposites: (A) T_g and T_m regions for PVIBE, (B) T_m region of ϵ -PL for PVIBE/ ϵ -PL blends, and (C) T_m region of ϵ -PL for PVIBE/ ϵ -PL/saponite clay nanocomposites.

1/0.03 powder is obtained from drying water solution including both ϵ -PL and saponite clay, so that the crystal form of ϵ -PL/saponite is significantly different from that of pristine ϵ -PL. Probably the T_m peak at 457 K is ascribed to the crystalline phase strongly interacted with clay layers; the clay layers protect against the melting of the crystalline phase until 457 K. After mixing with PVIBE in chloroform/methanol solution, the T_m peak is not observed at 457 K. This indicates that the strong interaction between ϵ -PL crystal and saponite clay is disappeared by blending with PVIBE. Therefore, it is not necessary to consider the strong interaction between ϵ -PL crystalline phase interface and saponite clay for the PVIBE/ ϵ -PL/saponite clay nanocomposites, and we can straightforwardly compare the effect of blending PVIBE on domain size and T_m of ϵ -PL for the blends with for the nanocomposites.

Figure 1C represents that the T_m values from PVIBE/ ϵ -PL/saponite clay = 10/3/0.09 to 10/5/0.15 are equal to 439 K with each other. In contrast, those of PVIBE/ ϵ -PL = 10/3 to 10/5 blends have the respective value. Namely, T_m values of blends depend on the composition but those of nanocomposites do not. For the PVIBE/ ϵ -PL/saponite clay = 10/1/0.03 and 10/2/0.06 nanocomposites, however, those T_m values depend on the composition as well as those for the PVIBE/ ϵ -PL = 10/1 and 10/2 blends. If the diluent effect is predominant, the shift tendency of T_m toward lower temperature with composition is reasonable for PVIBE/ ϵ -PL/saponite clay = 10/2/0.06 to 10/1/0.03. However, the constancy of T_m values for PVIBE/ ϵ -PL/saponite clay = 10/3/0.09 to 10/5/0.15 cannot be interpreted well. On the basis of the Gibbs–Thomson effect,¹ the same lamellar thickness exhibits the same T_m value. The DSC results shown in Figure 1C imply that the change of T_m is attributable to the lamellar thickness in the crystalline domain of ϵ -PL but not to the diluent effect by adding PVIBE.

Figure 2A shows the observed ^{13}C CPMAS NMR spectra of (a) PVIBE, (b) PVIBE/ ϵ -PL = 10/2, (c) PVIBE/ ϵ -PL/saponite = 10/2/0.06, (d) ϵ -PL, and (e) ϵ -PL/saponite clay = 1/0.03. Although the peak intensities are enhanced individually by CP, we ascertained the real contents of PVIBE/ ϵ -PL blends and nanocomposites by ^1H dipolar decoupling (DD) with MAS spectra. The spectrum of the ϵ -PL/saponite clay = 1/0.03 (e) shows that the relative ratio of broad lines is much more than

that of ϵ -PL (d). For example, the CH_2 peaks at the 20–40 ppm region, which consist of apparently four narrow peaks and broad lines, show much broader. This suggests that the degree of crystallinity decreased by adding saponite clay.

To investigate the crystallinity, we obtained the ^{13}C CPMAS NMR spectra separated into contributions arising from the crystalline (CR) and noncrystalline (NC) phases by basing on the differences in the intrinsic ^1H spin–lattice relaxation time in the rotating frame, which characterize the CR and NC phases.^{5,6} Figure 2B shows the expanded and separated spectra for the PVIBE/ ϵ -PL/saponite clay = 10/2/0.06 nanocomposites. Spectra (g) and (i) correspond respectively to the CR phase of CH–O–CH_2 carbons of PVIBE and C_αH carbon of ϵ -PL. Similarly, spectra (f) and (h) are attributed to those NC phases. The crystallinity is estimated from the relative contribution of the CR component of the whole ^{13}C CPMAS spectrum after a CP time of 800 μs . Since the peak integrals are distorted during the CP contact time, the values were corrected by using an individual CP efficiency. The crystalline domain size can be analyzed from the ^1H spin–diffusion rate between PVIBE and ϵ -PL.³

Figure 3 shows the ^1H spin–lattice relaxation (T_1^{H}) curves observed from both polymers in PVIBE/ ϵ -PL/saponite clay = 10/2/0.06 through well-resolved solid-state ^{13}C NMR signals: namely, the T_1^{H} curves were obtained from the signal intensity change occurring during the inversion recovery method via the CP transfer from ^1H to ^{13}C under the MAS condition. The broken straight lines represent T_1^{H} decays for each homopolymer before blending. The observed T_1^{H} decay plots (open circles: PVIBE; open triangles: ϵ -PL) are curved rather than straight. Similar curves were observed for every blend³ and every nanocomposite. It seems that the observed T_1^{H} decay of PVIBE deviates very slightly from that of the pure one. This is because the amount of PVIBE is much larger than that of ϵ -PL. The effect of the ^1H spin diffusion on the T_1^{H} decays depends on the proton molar fraction, so that the T_1^{H} decay of ϵ -PL is largely affected rather than that of PVIBE. Actually, even the theoretically fully averaged T_1^{H} decay appears very close to that of PVIBE as shown by broken-dotted line in Figure 3. The T_1^{H} decay of PVIBE hence ostensibly shows similar to that of pure PVIBE even though the influence of ^1H spin diffusion occurs

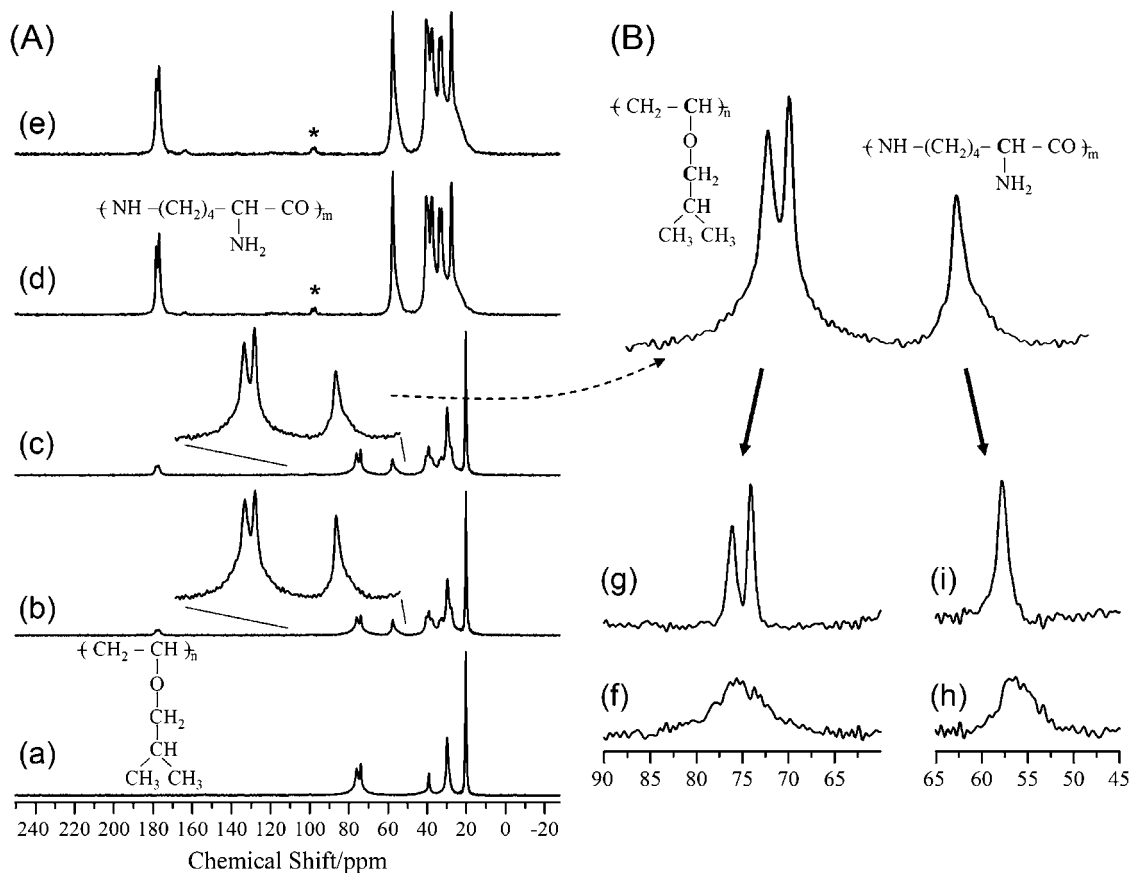


Figure 2. Observed ^{13}C CPMAS NMR spectra (A) of (a) PVIBE, (b) PVIBE/ ϵ -PL = 10/2 blend, (c) PVIBE/ ϵ -PL/saponite = 10/2/0.06 nanocomposite, (d) ϵ -PL, and (e) ϵ -PL/saponite clay = 1/0.03 powder. Expanded and separated ^{13}C CPMAS NMR spectra (B) for the PVIBE/ ϵ -PL/saponite = 10/2/0.06 nanocomposite based on differences in the ^1H rotating-frame relaxation times: CHOCH_2 peaks of PVIBE are on the left and C_αH peak of ϵ -PL on the right. Spectra (g, i) and (f, h) are attributed to the CR phase and the NC phase, respectively.

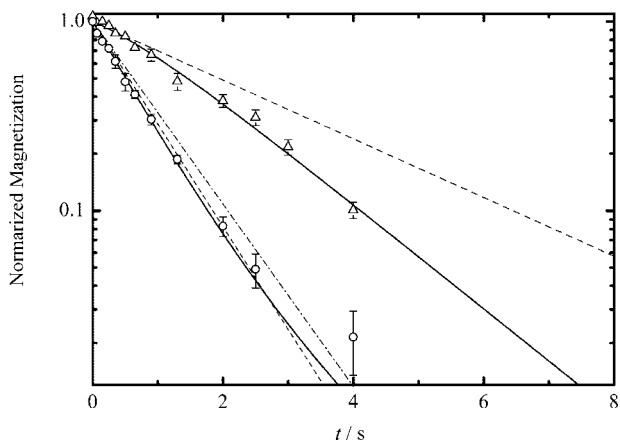


Figure 3. Observed T_1^{H} relaxation curves of the PVIBE/ ϵ -PL/saponite = 10/2/0.06 nanocomposite at 500 MHz resonance. The symbols of circle are PVIBE ($\text{CH}-\text{O}-\text{CH}_2$ carbon signal) and triangle ϵ -PL (C_αH carbon signal). Each solid line is calculated from the two-spin system model. The broken lines represent the relaxation curves of pure PVIBE ($T_1^{\text{H}} = 0.8$ s) and pure ϵ -PL ($T_1^{\text{H}} = 2.8$ s). The broken-dotted line indicates the fully averaged relaxation curve ($T_1^{\text{H}} = 0.9$ s) in the case of the extremely fast ^1H spin diffusion between PVIBE and ϵ -PL for 10/2 composition.

in both PVIBE and ϵ -PL wholly. For the PVIBE/ ϵ -PL/saponite clay = 10/2/0.06 nanocomposites, both T_1^{H} decays are successfully fitted by the simple and typical two-spin system as will be seen later.

If these blends and nanocomposites are homogeneous on a 20–50 nm level,^{7–9} the observed T_1^{H} relaxation of PVIBE will

coincide with that of ϵ -PL and both relaxation decays will be the same straight line (broken-dotted line in Figure 3) because of occurring the very fast ^1H spin diffusion between PVIBE and ϵ -PL domains. However, the observed T_1^{H} curves of PVIBE and ϵ -PL do not conform to the average decay. This indicates that PVIBE and ϵ -PL are heterogeneous on a scale of 20–50 nm. On the other hand, the observed T_1^{H} curves show the typical curvature in the case of insufficient ^1H spin-diffusion rate for a two-spin system.⁷ This also suggests that the nanocomposites are not completely phase separated, but several tens of nanometers size domains exist within the reach of ^1H spin interaction.

In the semicrystalline polymer case, furthermore, we can detect both relaxation curves of noncrystalline (NC) and crystalline (CR) phases. Actually, we observed a sharp ^{13}C signal which is attributed to the CR phase overlapped with a broad resonance ascribed to the NC phase, as shown in Figure 2B. However, the T_1^{H} curve obtained from the CR phase completely coincided with that obtained from the NC phase for both polymers, except for PVIBE/ ϵ -PL = 10/1 composition. For the PVIBE/ ϵ -PL = 10/1 blend and the PVIBE/ ϵ -PL/saponite = 10/1/0.03 nanocomposite, the T_1^{H} curve obtained from the CR phase of ϵ -PL was not in agreement with that of NC phase. These observations indicate that (1) blends and nanocomposites are not completely heterogeneous on a scale of several tens of nanometers size but an insufficient (intermediate) ^1H spin diffusion occurs to average out the relaxations, (2) there is very fast ^1H spin diffusion between the CR and the NC phases in each polymer except for PVIBE/ ϵ -PL = 10/1 composition, and thus (3) we can estimate the domain size by assuming the two-

spin system⁵ for PVIBE and ε -PL domains to analyze the observed T_1^H curves; protons in both CR and NC phases have the same spin temperature. For the PVIBE/ ε -PL/saponite = 10/1/0.03 nanocomposite, a three-spin system is adopted to analyze the observed T_1^H curves as same as that of the PVIBE/ ε -PL = 10/1 blend.³

The two- or three-spin systems for the PVIBE/ ε -PL blends and the PVIBE/ ε -PL/saponite nanocomposites are schematically illustrated in Figure 4. Figure 4A shows the two-spin system of which both ^1H spins of CR and NC regions have the same relaxation rate (spin temperature) for each polymer; thus, the two kinds of ^1H spin species are the protons of PVIBE and the protons of ε -PL.

To investigate the domain size from the ^1H spin-diffusion rate, it is very important to choose the appropriate model to reveal actual morphology. In the present case, both polymers are semicrystalline polymers, but the blends and nanocomposites do not show a eutectic temperature (Figure 1). A typical CR phase contains regularly aligned (lamellar) and small amount of disordered regions (interface), so that usually the CR region locates neighborhood of NC region by connecting with the interface. Therefore, a CR domain of ε -PL is surrounded by NC domains of ε -PL, and a similar criterion holds on PVIBE. Moreover, it is usual that the NC region of PVIBE interacts with that of ε -PL and not the CR region for semicrystalline polymer blends. The very fast ^1H spin diffusion between NC and CR regions in the respective polymers obscures the direct spin interaction between NC regions of PVIBE and ε -PL, so that the system can be assumed by the two kinds of ^1H spin species even though the several domains coexisted in these blends and nanocomposites. Thus, it is reasonable to assume the alternately aligned two domains of PVIBE (large domain) and ε -PL (small domain), which sizes are larger than several tens of nanometers scale, to explain the insufficient ^1H spin diffusion for T_1^H relaxations.

Figure 4B exhibits the three-spin system for ^1H spins among PVIBE, CR for ε -PL, and NC for ε -PL. For 10/1 composition, the amount of ε -PL is extremely limited so that a large quantity of PVIBE interacts with both CR and NC phases of ε -PL directly much easier than the other compositions. Consequently, the ^1H spin-diffusion rate between CR and NC phases in ε -PL is largely modulated and becomes no longer very fast.

The proton magnetizations $M_i(t)$ of i spin for two- and three-spin systems are expressed by eqs 1 and 2, respectively, as follows:⁷⁻⁹

$$\frac{d}{dt} \begin{pmatrix} M_A(t) \\ M_B(t) \end{pmatrix} = \begin{pmatrix} -\xi_A & f_A k \\ f_B k & -\xi_B \end{pmatrix} \begin{pmatrix} M_A(t) \\ M_B(t) \end{pmatrix} \quad (1)$$

where $\xi_A = K_A + f_B k$ and $\xi_B = K_B + f_A k$

$$\frac{d}{dt} \begin{pmatrix} M_1(t) \\ M_2(t) \\ M_3(t) \end{pmatrix} = \begin{pmatrix} -\xi_1 & f_1 k_{12} & f_1 k_{13} \\ f_2 k_{12} & -\xi_2 & f_2 k_{23} \\ f_3 k_{13} & f_3 k_{23} & -\xi_3 \end{pmatrix} \begin{pmatrix} M_1(t) \\ M_2(t) \\ M_3(t) \end{pmatrix} \quad (2)$$

where $\xi_1 = K_1 + f_2 k_{12} + f_3 k_{13}$, $\xi_2 = K_2 + f_1 k_{12} + f_3 k_{23}$, and $\xi_3 = K_3 + f_1 k_{13} + f_2 k_{23}$. Parameters f , K , and k represent ^1H molar fraction, intrinsic ^1H relaxation rate, and ^1H spin-diffusion rate, respectively. The simulated curves calculated from eq 1 for the PVIBE/ ε -PL/saponite = 10/2/0.06 nanocomposite are depicted by the solid lines in Figure 3 as an example. The obtained initial relaxation times are 0.73 s for PVIBE and 3.0 s for ε -PL. These values are in good agreement of those of pure polymers. The ^1H spin-diffusion rate, k , between PVIBE and ε -PL domains is obtained to be 0.38 s^{-1} . Those errors are within 10% of each

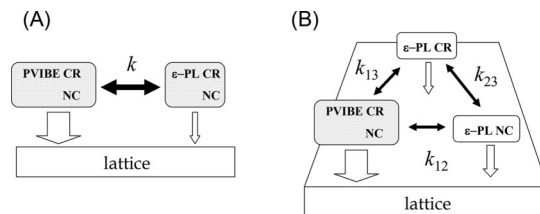


Figure 4. Schematic illustrations of (A) two- and (B) three-spin models. The large size of the arrow toward lattice represents the fast ^1H spin–lattice relaxation rate. A round box shows a single and the same spin system. The ^1H spin temperature of a crystalline phase (CR) is identical to that of an amorphous (noncrystalline) phase (NC) owing to extremely fast ^1H spin diffusion between both phases. For the three-spin system, there are three ^1H spin-diffusion rates, k_{12} , k_{13} , and k_{23} , among (1) PVIBE, (2) NC of ε -PL, and (3) CR of ε -PL.

Table 1. Obtained ^1H Spin-Diffusion Rates, k , and the Estimated Repeat Lengths, L , of both PVIBE and ε -PL Domains for the Blends and the Nanocomposites from the Formula $L = 2(D/\pi k)^{0.5}/(f_{\text{PVIBE}}f_{\varepsilon\text{-PL}})^a$

composition	$k \text{ (s}^{-1}\text{)}$	$L \text{ (nm)}$	$L_{\varepsilon\text{-PL}} \text{ (nm)}$	$x_C \text{ (\%)}$	$L_C \text{ (nm)}^c$
10/1	0.33^b	569	41	30	12
10/2	0.37	309	42	58	24
10/3	0.20	320	61	57	35
10/4	0.12	350	83	55	46
10/5	0.10	345	97	59	57
10/1/0.03	0.25^b	654	47	36	17
10/2/0.06	0.38	305	41	46	19
10/3/0.09	0.15	369	70	47	33
10/4/0.12	0.18	286	68	44	30
10/5/0.15	0.21	238	67	49	33

^a The crystallinity, x_C , of ε -PL is obtained from the spectral subtraction based on differences in the ^1H rotating-frame relaxation times during the spin-locking pulse.^{3,5,6} ^b The k values for PVIBE/ ε -PL = 10/1 and PVIBE/ ε -PL/saponite = 10/1/0.03 are obtained from the three-spin model among both spins of ε -PL noncrystalline and crystalline phases and PVIBE. The value is between the crystalline phases of ε -PL and PVIBE. ^c L_C is calculated from $L \times f_{\varepsilon\text{-PL}} \times x_C/100$.

value.

Instead of the two-spin model, we may fit the observed T_1^H curves by a dispersion model, which ε -PL disperses in the large amount of PVIBE that ε -PL is in close proximity to PVIBE. In such a case, however, the initial relaxation time of ε -PL will be very short when we use the two-spin model for simulation because the molecular motion is drastically changed by surrounding PVIBE. The estimated initial value of ε -PL is comparable to that of pure one. Thus, we concluded that simple alternating-domain (two-spin) model is plausible for this system. The repeating unit length, L , can be estimated from the relation of $L = 2D^{0.5}(\pi k)^{-0.5}(f_{\text{PVIBE}}f_{\varepsilon\text{-PL}})^{-1}$: D is the ^1H spin-diffusion coefficient for the PVIBE/ ε -PL system ($380 \text{ nm}^2 \text{ s}^{-1}$) and obtained from the ^1H spin–spin relaxation time.⁸⁻¹²

Table 1 lists the obtained k , the estimated L , the degree of crystallinity, x_C , of ε -PL, and the domain size which is related to the total lamellar thickness, L_C , of the crystalline phase of ε -PL. The x_C values of nanocomposites are smaller than those of the PVIBE/ ε -PL blends by about 10%, except for the PVIBE/ ε -PL/saponite = 10/1/0.03 nanocomposite. The crystallinity of ε -PL/saponite was also decreased from ca. 60% until ca. 42%. This indicates that the mixing of saponite clay acts as an inhibitor for growing of lamellar layer in crystalline phase of ε -PL; in fact, the enthalpy of ε -PL after adding saponite clay decreases and T_m becomes 442 K from 445 K (Figure 1C).

There exists the good relationship between the decrease of L_C values and the depression of the melting point with decreasing of ε -PL for blends. This has already been discussed in the previous paper.³ On the other hand, the L_C values for

PVIBE/ ϵ -PL/saponite = 10/3/0.09 to 10/5/0.15 exhibit the same value of 30–33 nm within an error of 10%. For further PVIBE rich compositions, L_C values decreases with PVIBE as well as those of blends. The L_C values for PVIBE/ ϵ -PL/saponite = 10/3/0.09 to 10/5/0.15 is comparable to that for the PVIBE/ ϵ -PL = 10/3 blend (35 nm). It is also interesting and surprising that the T_m values of the PVIBE/ ϵ -PL/saponite = 10/3/0.09 to 10/5/0.15 nanocomposites show the same value of 439 K with each other. Furthermore, this value is in excellent agreement with that of the PVIBE/ ϵ -PL = 10/3 blend, 440 K. For PVIBE/ ϵ -PL = 10/2 or 10/1 compositions, a similar relationship also remained; that is, the T_m value depends on the L_C value. These results clearly prove that the T_m value is governed by the lamellar thickness in crystalline domain not by the diluent effect in this PVIBE/ ϵ -PL system.

Here, we have to discuss the L_C value estimated from the ^1H spin-diffusion analysis in detail because it is disputable whether the calculated value is really related to the single lamellar thickness or not. There are two possibilities for the lamellar thickness in the case of the same crystallinity. One is that the lamellar thickness does not change but the amount of lamellar decreases with decreasing of the domain size. Another one is that the thickness of the single lamellar layer decreases with decreasing of the crystalline domain size of ϵ -PL but the amount increases in the crystalline phase to keep the constant crystallinity. In the latter case, T_m changes as expected by the estimated L_C value and obeys the Gibbs–Thomson relation. On the contrary, if the actual morphology is similar to the former condition, the decreasing of T_m may be explained by the diluent effect of adding PVIBE. Actually, we cannot distinguish apparently between the diluent effect and the Gibbs–Thomson effect from the L_C estimation only for the blends. However, it is also true that the diluent effect cannot explain the constancy of T_m observed for the nanocomposites. The decrease of the lamellar thickness gives unambiguous solution of the shift and

the constancy of T_m values observed for both blends and nanocomposites, if the estimated L_C value is comparable to a summation of a single lamellar layer thickness.

Consequently, we explained the phenomenon of T_m shift observed in PVIBE/ ϵ -PL systems with the Gibbs–Thomson effect by comparing the L_C estimation of both blends and nanocomposites. This simple L_C estimation from the ^1H spin diffusion through $T_1\rho$ curve is useful to detect the lamellar thickness. However, it is also noted that this observation may not be always true because the estimated L_C value does not relate to the thickness of a single lamellar layer but always gives the total thickness. In these PVIBE/ ϵ -PL blends and PVIBE/ ϵ -PL/saponite clay nanocomposites, this observation successfully showed the evidence of the relationship between the lamellar thickness and the T_m shifts.

References and Notes

- (1) Strobl, G. R. *The Physics of Polymers*; Springer-Verlag: Berlin, 1997.
- (2) Utracki, L. A. *Polymer Alloys and Blends - Thermodynamics and Rheology*; Carl Hanser-Verlag: Munich, 1989.
- (3) Asano, A.; Murata, Y.; Kurotsu, T. *E-J. Soft Mater.* **2007**, *3*, 1–8.
- (4) Asano, A.; Tanaka, C.; Murata, Y. *Polymer* **2007**, *48*, 3809–3816.
- (5) VanderHart, D. L.; Pérez, E. *Macromolecules* **1986**, *19*, 1902–1909.
- (6) VanderHart, D. L.; Asano, A.; Gilman, J. W. *Chem. Mater.* **2001**, *13*, 3781–3795.
- (7) Stejskal, E. O.; Schaefer, J.; Sefcik, M. D.; McKay, R. A. *Macromolecules* **1981**, *14*, 275–279.
- (8) Asano, A.; Takegoshi, K. In *Solid State NMR of Polymers*; Ando, I., Asakura, T., Eds.; Elsevier: Amsterdam, The Netherlands, 1998; pp 351–414.
- (9) Asano, A. In *Modern Magnetic Resonance*; Webb, G. A., Ed.; Springer: The Netherlands, 2006, Vol. 1, pp 627–631.
- (10) VanderHart, D. L.; McFadden, G. B. *Solid State Nucl. Magn. Reson.* **1996**, *7*, 45–66.
- (11) Demco, D. E.; Johansson, A.; Tegenfeldt, J. *Solid State Nucl. Magn. Reson.* **1995**, *4*, 13–38.
- (12) Assink, R. A. *Macromolecules* **1978**, *11*, 1233–1237.

MA801536N